The Cause of Faint Coronal Jets from Emerging-Flux Regions in Solar Coronal Holes

Abigail R. Harden[1], Navdeep K. Panesar[2], Alphonse C. Sterling[2], Ronald L. Moore[2,3]

[1] Agnes Scott College, [2] NASA Marshall Space Flight Center, [3] Center for Space Plasma and Aeronomic Research, University of Alabama in Huntsville

Contact: aharden@agnesscott.edu

Abstract

Coronal jets are transient thin bursts of magnetically channeled solar material from the surface into the corona. They are brightest at their base, with a bright point (jet bright point, JBP) at an edge of the base. Early studies (Shibata et al. 1992) suggested that jets result from magnetic flux emergence: a small bipole emerges into unipolar ambient field, driving the jet and forming the JBP via interchange reconnection. More recent studies, using higher-cadence, higher-resolution, and broader wavelength coverage than before, show that prominent coronal jets are usually driven by a minifialment eruption (Sterling et al. 2015), and that, rather than flux emergence, flux cancelation usually prepares and triggers the eruption (Panesar et al. 2016). Here, we analyzed eight emerging flux regions to determine whether the emerging flux directly drove any coronal jets. We used EUV images from the Solar Dynamics Observatory (SDO)/Atmospheric Imaging Assembly (AIA) (in 304, 171, 211, 193, and 94 Å channels), and magnetograms from SDO/Helioseismic & Magnetic Imager (HMI). All eight regions produced jet-like features that were weak in intensity (“faint jets’’), by which we mean they were so faint that we likely would not have identified them as jets had we initially searched for jets in AIA movies alone (as in, e.g., Panesar et al. 2016, Moore et al. 2013) without knowing whether the base was an emerging bipole. In seven of the eight regions, all jets (faint or prominent) erupted from locations where one leg of the emerging bipole was evidently canceling with an ambient opposite-polarity flux clump. The eighth case, the one that had the fastest flux emergence, possibly made faint jets by the flux-emergence mechanism, but these too might instead have resulted from flux cancelation.

Introduction

Coronal jets are thin streams of plasma which flow out along magnetic field lines in the corona. They can be found in various solar environments including active regions, coronal holes, and the quiet sun (Raoufi et al. 2016). It is generally agreed upon that some form of magnetic reconnection drives these jets. Some studies suggested flux emergence to be the main driver of coronal jets (Shibata et al. 1992), while others have found erupting minifilaments to be the primary driver of coronal jets (e.g., Sterling et al. 2015, Panesar et al. 2018). Two discussed mechanisms for coronal jet formation are emerging flux and flux cancelation, shown in Figure 1 and Figure 2 respectively.

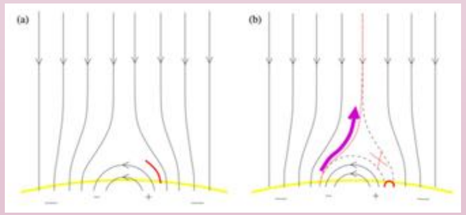

Sterling et al. 2015

Figure 1
The initial condition (a) features an emerging bipole in a unipolar ambient field. A plasma current sheet (red) forms at the null region between opposite polarity fields. Flux emergence of the bipole triggers reconnection at the red cross in (b). This results in a new closed loop, which is the JBP (red loop in (b)), and new connections with the ambient field along which plasma (purple arrow) flows.

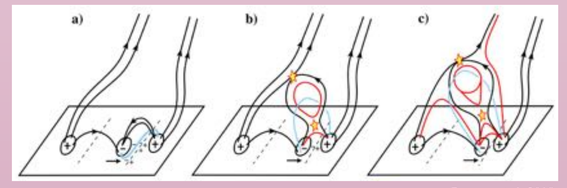

Panesar et al. 2018

Figure 2
Panel (a) shows the highly sheared minifilament field (blue) sits over the neutral line (dashed lines) between two opposite polarity flux patches, which are migrating towards each other. As these flux patches cancel at the neutral line (b), the highly sheared field holding the minifilament becomes unstable, causing the minifilament to erupt over the small bipole. This eruption triggers internal reconnection (lower star (b) & (c)), creating the JBP (lower red line (b) & (c)). The JBP forms under where the minifilament had been rooted prior to eruption. The minifilament carrying field also undergoes external/interchange reconnection with the ambient field (upper star (b) & (c)), creating two new connections. These connections are shown as the closed red loop across the base of the bipole and the open red line in (c). Heated material flows along the latter of these connections, forming the jet spire.

Motivations

We investigate in detail eight emerging flux regions from the start to end of emergence using SDO/AIA data. We tracked changes of the emerging bipole in the photospheric magnetic field using line of sight magnetograms from SDO/HMI. We found faint coronal jets in the emerging flux regions, and sought to determine their cause. Table 1 shows our eight randomly selected emerging flux regions.

Methods

We first identified emerging flux regions using HMI line-of-sight magnetograms. We then searched for faint jets in AIA EUV images. We removed solar rotation and coaligned the data sets using SolarSoft routines. We then made movies at two and three minute cadences for AIA and HMI respectively. To better see the faint jet spires, we made reversed color images and we made summed images by adding two adjacent images. We also made summed HMI magnetograms in the same way to enhance weak magnetic field regions. We used AIA 211 Å data to make time-distance plots of the base of the emerging bipole. These plots show the growth of the emerging bipole. We also made flux plots using this HMI data. We carefully checked each HMI frame to make sure no flux crossed the chosen boundaries. The minority flux was typically measured since it is easier to isolate from the ambient field. These plots show the general strength of the magnetic field over time, which allowed us to determine over what period of time flux was emerging and at what rate. Approximate jet speeds are the Plane-of-sky speed taken along the jet spire in summed AIA 193 Å images (some exceptions are noted in Table 1).

Figure 3
Pannels (a)-(c) show the onset, peak, and end of the first faint jet in 193 Å reversed color images. Panels (d)-(f) show HMI magnetograms with magnetic field strength ± 75 G of the same region. Panel (d) shows the region before flux cancelation starts, (e) shows the cancelling region, (f) shows the region after the negative flux patch has completely canceled. The white and yellow boxes in (d) is referenced in Figures 4a and 4b, respectively. Arrows point to the canceling flux patch in (e). This faint jet shoots out with an average speed of 90 km s^{-1}.

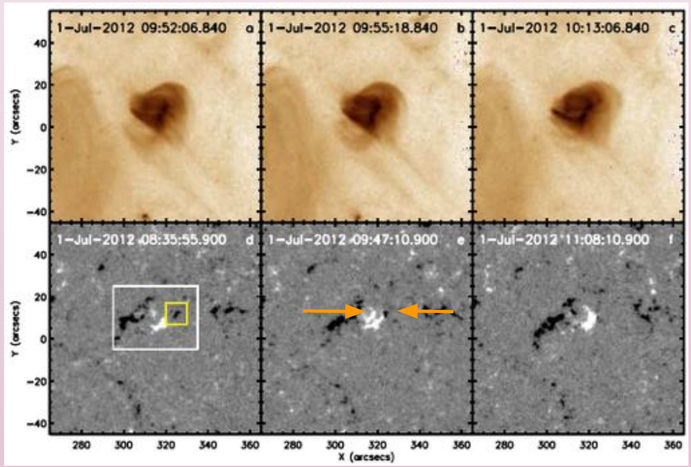

Figure 4
Panels (b) and (c) are flux plots with $\log_{10}$ scaling on the y-axis and the dashed vertical lines at 9:48 and 10:52 indicate start time of faint jets J2 and J3. Plot (b) shows the positive flux curve, bounded by the white box in Figure 3 (d). Plot (c) shows the negative flux as a function of time computed inside the yellow box in Figure 3 (d).

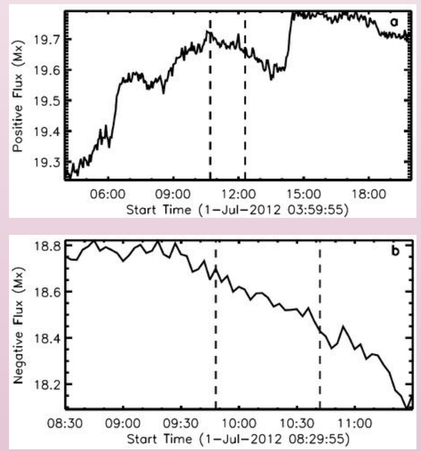

Figure 5
Panels (a)-(c) shows the onset, peak, and end of J23 in 193 Å reversed color images. The arrow in (b) points to the faint jet spire. Panels (d) & (e) are HMI magnetograms with intensity ± 75 G and show the region prior to and during flux emergence, and the black box in (d) is referenced in Figure 6. Panel (f) shows the same image as panel (a) but with contours overlaid. The contour level is ± 50 G with red and green representing positive and negative respectively. This faint jet has an average speed of 90 km s^{-1}.

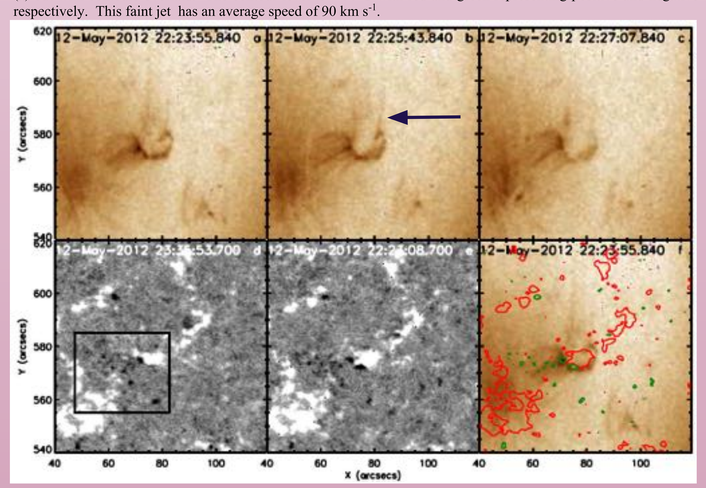

Figure 6
Panel (b) shows the flux plot of the region over the entire event, which is represented by the black box in Figure 5 (d). Panel (c) shows the flux plot of the same region just over the first hour of the event. Both plots have a $\log_{10}$ on the y-axis, and the dashed vertical lines indicate the time of jet onset at 22:24, 22:33, and 22:38

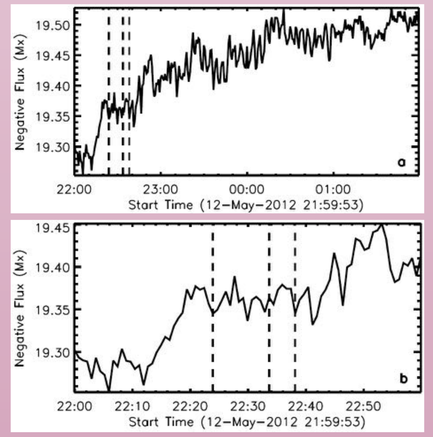

Results

We studied eight emerging flux regions, and found 25 faint coronal jets which occurred during the emerging flux period. We did not find any faint jets which occurred after the bipole had finished emerging. All of these jets are shown in Table 1, and we show Jet 2 and Jet 23 in detail as examples in Figure 3 and Figure 5 respectively. We found that out of 25 jets occuring during times of emerging flux, 21 were clearly driven by flux cancelation, as shown in Figure 2. Jets 23, 24, and 25 are candidates for jets made by the flux-emergence mechanism. In 21 of these jets, there was clear flux cancelation with the ambient coronal field at one leg of the emerging bipole. The jets in event 8 (J23, J24, & J25) may have been made by the flux-emergence mechanism, but we cannot say this with certainty. The magnetic flux in this event was very close to the noise level, so there may have been some weak cancelation happening at this time that we could not see. Here, we have shown jets from events E2 and E8, which represent the typical faint jet from flux-cancelation and flux-emergence respectively. Event E2 (Figure 3) has two faint jets during its emerging flux period, both occurring from the same neutral line. Flux cancelation at the neutral line between one (positive) leg of the emerging bipole and a small patch of the ambient (negative) field triggers the first faint jet (J2), and continual cancelation of the same flux patches triggers the second jet (J3) about an hour later. The small patch of ambient field has completely cancelled at the completion of J3, and as there were no more faint jets from this region. Event E8 (Figure 5) produced three jets which may have been caused by flux-emergence. There is no detectable flux cancelation before or during the first jet (J23), although there may be some weak cancelation close to the noise level during Jets 24 and 25.

Table 1 Physical Parameters of Observed Faint Jets

Emerging Flux Region No.	Start Time (UT)	End Time (UT)	No. of Faint Jets	Jet No.	Time (UT)	Duration (min.)	Triggered by Flux Emergence?	Speed (km s^{-1})
E1	21:00 June 30 2012	10:00 July 1 2012	1	J1	21:30	2 ± 1	Ambiguous	90 ± 30
E2	04:00 July 1 2012	20:00 July 1 2012	2	J2	09:48	15 ± 5	N	90 ± 5
				J3	10:52	13 ± 4	N	90 ± 10
E3	15:00 July 1 2012	08:00 July 2 2012	2	J4	18:17[3]	9 ± 2	N	-
				J5	18:41[3]	4 ± 1	N	-
E4	20:00 January 9 2015	18:00 January 11 2015	3	J6	12:45	7 ± 5	N	180 ± 65 [6]
				J7	19:08	16 ± 10	N	80 ± 25 [6]
				J8	20:46	32 ± 6	N	175 ± 45 [6]
E5	20:00 January 9 2015	18:00 January 11 2015	10	J9	10:19[3]	9 ± 2	N	235 ± 70
				J10	10:31[3]	6 ± 3	N	200 ± 10
				J11	10:40[3]	2 ± 1	N	120 ± 30
				J12	10:42[3]	9 ± 2	N	160 ± 10
				J13	10:58[4]	11 ± 3	N	115 ± 10
				J14	11:10[4]	8 ± 3	N	100 ± 10
				J15	11:23	13 ± 3	N	110 ± 10
				J16	12:09[5]	8 ± 2	N	130 ± 10
				J17	12:20[5]	8 ± 1	N	120 ± 10
				J18	17:24	10 ± 4	N	35 ± 10 [7]
E6	06:00 January 31 2017	06:00 February 1 2017	3	J19	08:16	4 ± 2	N	85 ± 10
				J20	08:26	10 ± 3	N	145 ± 5
				J21	09:04	7 ± 1	N	135 ± 10
E7	03:30 February 27 2011	10:30 February 27 2011	1	J22	04:31	11 ± 5	N	80 ± 20
E8	22:00 May 12 2012	02:00 May 13 2012	3	J23	22:24	3 ± 1	Y	90 ± 10
				J24	22:33[3]	3 ± 1	Y[8]	90 ± 10
				J25	22:38[3]	2± 1	Y[8]	100 ± 10

Notes
- [1,2,3,4,5] Pairs of jets originating from the same neutral line.
- [6] Speeds not calculated from summed images.
- [7] Jets are part of a cascading eruption.
- [8] Weak cancelation goes on at the edges of the majority-flux patch.

Conclusions

We studied eight emerging flux regions, which produced a total of 25 faint jets. These jets are significantly dimmer than the typical coronal jet, and would likely not have been noticed had we not deliberately searched for them in emerging flux regions. The jets in 7 of these events were all clearly made by the flux-cancellation mechanism. We found that the event with the fastest flux emergence may have produced jets via the flux-emergence mechanism. The average duration of the faint jets is 10 minutes, which is comparable to the duration of X-ray jets (Savcheva et al. 2007 & Panesar et al. 2016b), although the average duration of the faint jets which may have been driven by flux-emergence is only 3 minutes. The average speed of the faint jets is 125 km s^{-1}.

References

Moore, R. L.,Sterling,A. C., Falconer, D. A., & Robe, D. 2013, ApJ, 769, 134
Panesar, N. K., Sterling, A. C., & Moore, R. L., P. Chakrapani, 2016, ApJL, 822, L23
Panesar, N. K. et al. 2017 ApJ 844 131
Panesar, N. K. et al. 2018 ApJ 853 189
Raouafi, N. E., Patsourakos, S., Pariat, E., et al. 2016, SSRv, 201, 1
Savcheva, A., Cirtain, J., Deluca, E. E., et al. 2007, PASJ, 59, 771
Sterling, A. C., Moore, R. L., Falconer, D. A., & Adams, M. 2015, Nature, 523, 437
Shibata, K. et al. Observations of x-ray jets with the Yohkoh soft x-ray telescope. Publ. Astron. Soc. Jpn.44,173L–179L (1992).

Acknowledgments

This research was conducted thanks to the REU program funded by NSF and hosted by the University of Alabama in Huntsville and NASA’s Marshall Space Flight Center with additional support from the NASA HGI and NASA/MSFC NPP Program. This material is based on work supported by the National Science Foundation under Grant No. AGS-1460767.